

# Gamma Ray Astronomy with ARGO-YBJ

Silvia Vernetto (on behalf of the ARGO-YBJ Collaboration)

*IFSI-INAF, Corso Fiume 4 10133 Torino - Italy*  
*INFN Sezione di Torino, Via Pietro Giuria 1, Torino - Italy*

**Abstract.** ARGO-YBJ is the first EAS detector combining a very high mountain altitude (4300 m a.s.l.) to a “full coverage” detection surface. These features allow ARGO-YBJ to work with an energy threshold as low as a few hundreds GeV. The high duty cycle and the large field of view ( $\sim 2$  sr) make ARGO-YBJ suitable to monitor the gamma ray sky, searching for unknown sources and unexpected events, like Active Galactic Nuclei flaring episodes or high energy Gamma Ray Bursts.

In this paper we present the first observations of ARGO-YBJ concerning gamma ray astronomy, in particular the detection of the Crab Nebula and the blazar Markarian 421 during the 2006 and 2008 outbursts, and the results of a search for Gamma Ray Bursts emission in the GeV energy range using the scaler mode technique.

**Keywords:** Cosmic rays, Gamma rays, Air showers, Gamma ray sources, Gamma Ray Bursts

**PACS:** 96.50.sd, 95.55.Vj, 98.58.Mj, 98.54.Cm

## THE DETECTOR

ARGO-YBJ is a “full coverage” air shower detector specially designed to work with an energy threshold of a few hundreds GeV, located at the Yangbajing Cosmic Rays Laboratory (Tibet, P.R. China, lat=30.1°N, long=90.5°E) at an altitude of 4300 m above the sea level.

The high duty cycle and the large field of view ( $\sim 2$  sr) make ARGO-YBJ an instrument complementary to Cherenkov Telescopes in monitoring the gamma ray sky, in particular suitable to search for unknown sources and unexpected events, like Active Galactic Nuclei flaring episodes or high energy Gamma Ray Bursts.

ARGO-YBJ consists of a  $74 \times 78$  m<sup>2</sup> “carpet” realized with a single layer of Resistive Plate Counters (93% of active area) surrounded by a partially instrumented ( $\sim 40\%$ ) “sampling ring”, for a total active area of  $\sim 6700$  m<sup>2</sup>[1].

The detector is logically divided into 154 clusters, 130 of them forming the central carpet and 24 the sampling ring (see Fig.1). The cluster, consisting of a set of 12 RPCs, is the basic DAQ unit of the detector. Signals from each RPC are picked-up by 10 electrodes of dimension  $56 \times 62$  cm<sup>2</sup> (the “pads”) which provide the space-time pattern of the shower front with a time resolution of  $\sim 1$  ns. Each pad is segmented into 8 strips ( $62 \times 7$  cm<sup>2</sup>) which count the number of particles hitting the pad itself.

In order to extend the measurable primary energy range up to the PeV region, the RPCs are equipped with 2 large size pads ( $140 \times 125$  cm<sup>2</sup>), providing a signal of amplitude proportional to the number of particles.

The detector will be covered by a 0.5 cm thick layer of lead, in order to convert a fraction of the secondary gamma rays to charged particles and to reduce the time spread of the shower front, increasing the angular reso-

lution.

ARGO-YBJ operates in two independent acquisition modes: the “shower mode” and the “scaler mode”.

In “shower mode” all showers giving a number of fi red pads  $N_{pad} \geq N_{trig}$  in the central carpet during a time window of 420 ns are recorded. The spatial coordinates and the time of any fi red pad are then used to reconstruct the position of the shower core and the arrival direction of the primary[2].

To perform the time calibration of the 18480 pads, a software method has been developed[3].

The current trigger requires  $N_{trig} = 20$ , corresponding to a primary gamma ray energy threshold of a few hundreds GeV, the precise value depending on the source spectrum and on the zenith angle of observation. With this trigger condition, the event rate is  $\sim 4$  kHz.

Fig. 1 reports an example of a shower detected by the central carpet, showing the capability of ARGO-YBJ to provide a detailed view of the shower front.

In “scaler mode” the counting rates of each cluster are recorded every 0.5 s for 4 different levels of coincidence inside the cluster:  $\geq 1$ ,  $\geq 2$ ,  $\geq 3$ ,  $\geq 4$  pads, with a coincidence time window of 150 ns. The counting rates per cluster are respectively  $\sim 40$  kHz,  $\sim 2$  kHz,  $\sim 300$  Hz and  $\sim 120$  Hz, for the 4 coincidence levels.

This measurement allows the detection of secondary particles from very low energy showers ( $E > 1$  GeV) reaching the ground in a number not sufficient to trigger the detector operating in shower mode. In scaler mode the primary arrival directions are not reconstructed and the data are used to search for transient phenomena such as Gamma Ray Bursts or solar Ground Level Enhancements, and to study cosmic ray modulations due to the solar activity.

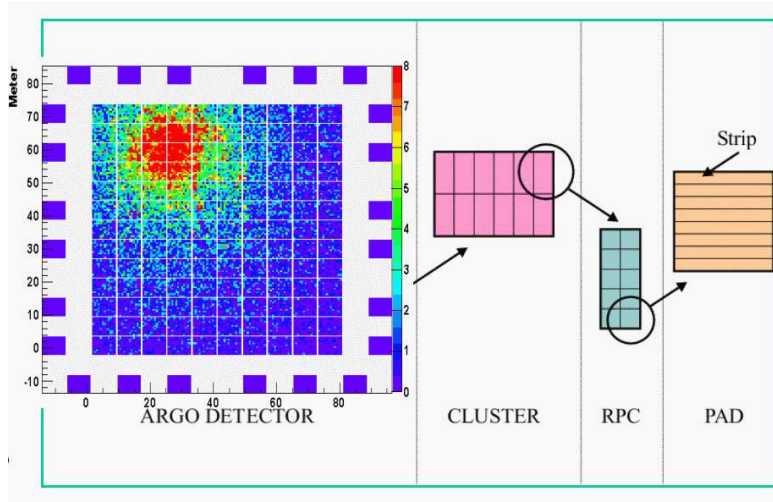


**FIGURE 1.** Layout of the ARGO-YBJ experiment, with a detected shower superimposed to the central carpet. Each point represents a fired pad. Different colours indicate the number of fired strips per pad.

From December 2004 to April 2007, during the detector installation, ARGO-YBJ has collected data for some limited periods of time using subsets of the detector. Since November 2007 the whole detector is in data taking with a duty cycle  $\geq 85\%$ .

## ANGULAR RESOLUTION

The angular resolution and the pointing accuracy of the detector have been evaluated by using the Moon shadow, i.e. the deficit of cosmic rays in the Moon direction. The Moon shadow is an important tool for ground-based detectors. In fact the shape of the shadow provides a measurement of the detector point spread function, and its position allows to find out possible pointing biases.

In addition, due to the geomagnetic field, positively charged particles are deflected towards the East by an angle of  $\Delta\phi \sim 1.6^\circ/E(\text{TeV})$ , where  $E$  is the particle energy. This effect produces a displacement of the shadow towards the West with respect to the Moon position and smears the shape in the East-West direction, especially at low energies. The observation of the displacement of the Moon provides a check of the relation between the shower size and the primary energy.

ARGO-YBJ in its final configuration observes the Moon shadow with a sensitivity of about 10 standard deviations per month for events with a multiplicity  $N_{pad} \geq 40$  and zenith angle  $\theta < 50^\circ$ , corresponding to a proton median energy of  $\sim 1.8$  TeV.

Fig.2 shows the Moon shadow obtained in 802 hours of measurements, from December 2007 to August 2008, for events with  $N_{pad} \geq 40$ . A deficit of  $\sim 26$  standard deviations is visible, slightly shifted towards the West by

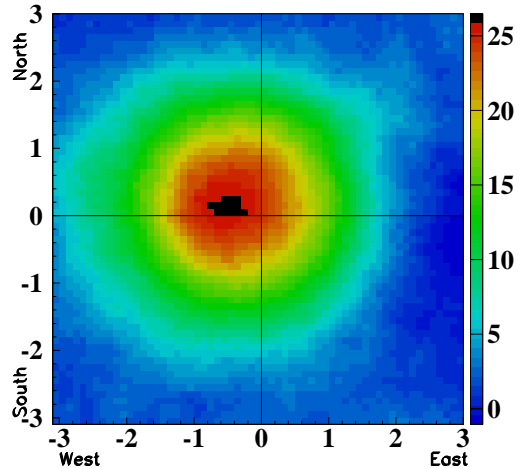


**FIGURE 2.** Map of the Moon region obtained in 802 hours of observation, for events with  $N_{pad} \geq 40$ . The colour scale shows the significance of the deficit in standard deviations. The axes report the distance in degrees from the Moon position. The shift towards the West is due to the deflection of cosmic rays by the geomagnetic field.

the geomagnetic field.

The upper panel of Fig. 3 shows the shift of the shadow in the East-West direction obtained with the data taken in different time periods, as a function of the minimum pad multiplicity on the central carpet, compared with the shift expected by a Monte Carlo simulation that propagates protons in the Earth-Moon system. The agreement is quite good, even in 2006 and 2007 data, when the detector was still in installation and debugging phase.

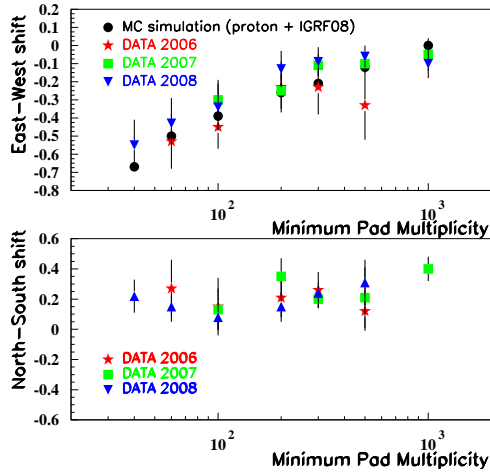


**FIGURE 3.** Shift of the Moon shadow (in degrees) with respect to the Moon position, as a function of the minimum pad multiplicity, in the East-West direction (upper panel) and North-South direction (lower panel).

The lower panel of the same figure shows the shadow shift in the North-South direction. According to simulations, given the ARGO-YBJ geographic location, this shift should be equal to zero. The observed shift of  $\sim 0.2^\circ$  towards the North is due to a systematic pointing error that we are currently investigating.

Fig.4 shows the angular resolution of the detector for proton showers as a function of the minimum pad multiplicity, obtained by the study of the Moon shadow profile in the North-South direction, where the geomagnetic field effect is negligible. The data show a good agreement with Monte Carlo simulation.

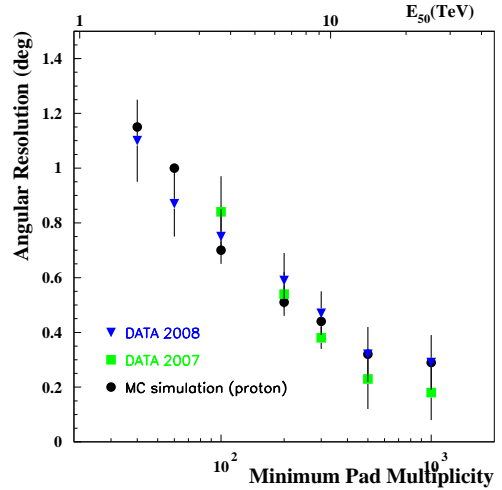
The Sun too casts a shadow on the cosmic rays background, but the shadow appears more smeared because of the particle deflection by the interplanetary magnetic field, whose intensity is related to the solar activity. The Sun shadow is more visible during periods of low solar activity, like in years 2006-2008.

Fig.5 shows the Sun shadow obtained in 954 hours of measurements, from December 2007 to August 2008, for events with  $N_{pad} \geq 40$ . A deficit of  $\sim 24$  standard deviations is visible. In addition to the West shift due to the geomagnetic field, the shadow is slightly distorted by the interplanetary magnetic field.

## THE CRAB NEBULA

Among the steady TeV gamma ray sources, the Crab Nebula is the most luminous and it is used as a standard candle to check the detectors sensitivity.

At the Yangbajing latitude the Crab culminates at



**FIGURE 4.** Angular resolution for protons, as a function of the minimum pad multiplicity, obtained by the Moon shadow observation. The upper axis reports the median energy of protons corresponding to the given pad multiplicity.

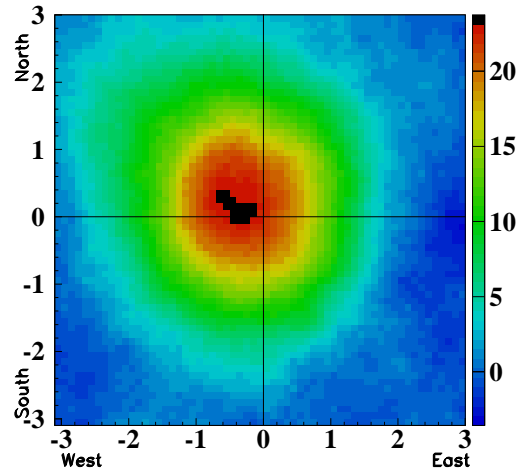


**FIGURE 5.** Map of the Sun region obtained in 954 hours of observation, for events with  $N_{pad} \geq 40$ . The colour scale shows the significance of the deficit in standard deviations. The axes report the distance in degrees from the Sun position. The shift and the distortion of the shadow are due to the deflection of cosmic rays by the terrestrial and interplanetary magnetic fields.

zenith angle  $\theta_{culm} = 8.1^\circ$  and is observable every day for 5.8 hours with a zenith angle  $\theta < 40^\circ$ .

Fig.6 shows the map of the Crab Nebula region obtained by ARGO-YBJ in its final configuration, using the events with  $N_{pad} \geq 40$  and  $\theta < 40^\circ$  recorded in 1133 on-source hours, equivalent to  $\sim 194$  transits of the source (from 2007 December 13 to 2008 August 17).

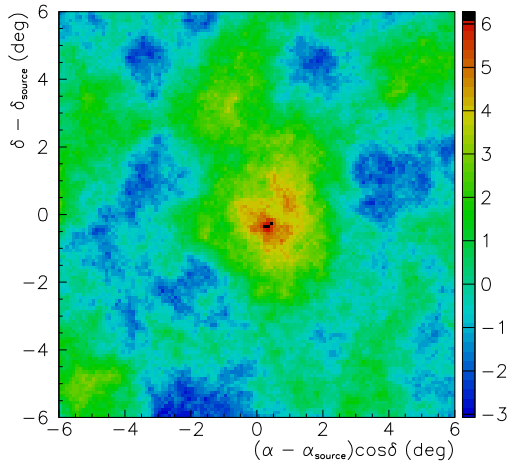


**FIGURE 6.** Map of the Crab Nebula region in 194 days of measurements, obtained with showers with  $N_{pad} \geq 40$ . The colour scale shows the significance of the signal in standard deviations.

The Crab is visible with a statistical significance of more than 6 standard deviations.

The map has been obtained by “smoothing” with a window of radius  $r=1.2^\circ$  the original event map with bins of size  $0.1^\circ \times 0.1^\circ$ . The chosen value of  $r$  corresponds to the radius of the circular window that maximizes the signal to noise ratio, according to simulations.

The median primary energy of events with  $N_{pad} \geq 40$  from a source with the Crab spectrum slope and following the Crab path in the sky is  $\sim 1.1$  TeV. We note that this is the first time that an air shower experiment detects photons from a point source at such a low energy.

The number of gamma rays detected per day is  $165 \pm 35$  for  $N_{pad} \geq 40$ , and  $19 \pm 7$  for  $N_{pad} \geq 200$ , in agreement with simulations.

No event selection and no gamma-hadron discrimination have been used in this analysis. An increase of the sensitivity of a factor  $\sim 1.5$  is expected by using “topology-based” selection criteria to reject a fraction of background protons, currently under study[4].

## MARKARIAN 421

Markarian 421 is one of the closest blazars and the first extragalactic source observed in the TeV energy range. It is extremely variable at any wavelength. The X-ray and TeV fluxes are often correlated, and in many occasions the latter becomes several times larger than the Crab Nebula one.

As the Crab Nebula, Mrk421 culminates at the ARGO-YBJ location with a zenith angle  $\theta_{culm} = 8.1^\circ$ , but it is

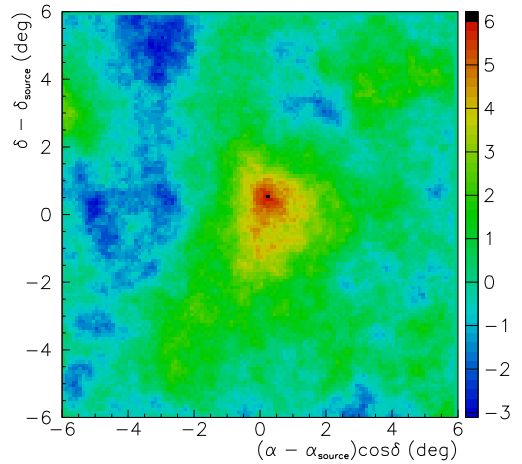


**FIGURE 7.** Map of the Mrk421 region during the outburst of July-August 2006 obtained with showers with  $N_{pad} \geq 40$ . The colour scale shows the significance of the signal in standard deviations.

observable every day for 6.3 hours with a zenith angle  $\theta < 40^\circ$ .

In summer 2006 Mrk421 underwent an active period with a rather strong increase of the X-ray flux[5]. The 2006 summer outburst was not observable by Cherenkov telescopes, being the source high in the sky during the daytime.

ARGO-YBJ observed Mrk421 during 109 hours from July 9 to September 2, just at the end of the installation of the central carpet, during the debugging phase of the detector.

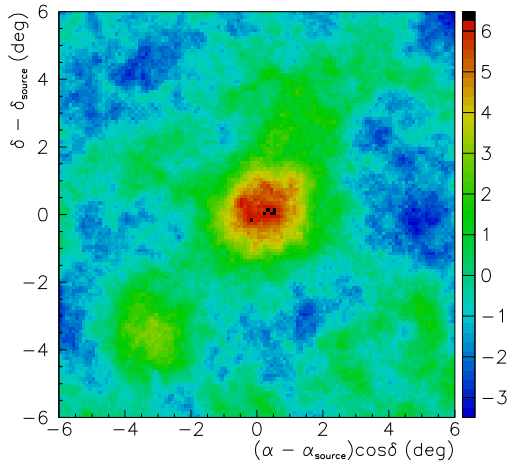
Fig. 7 shows the map of the region around the source, obtained with all events with  $N_{pad} \geq 40$  and  $\theta < 40^\circ$ . The significance of the signal is  $\sim 6$  standard deviations. Assuming a spectrum slope similar to the Crab Nebula one, the median energy of the events is  $\sim 1.1$  TeV and the average flux is  $\sim 3$  Crab units.

In 2008 Mrk421 had many very active periods, with the maxima of X-ray emission around days 40, 80 and 160[5].

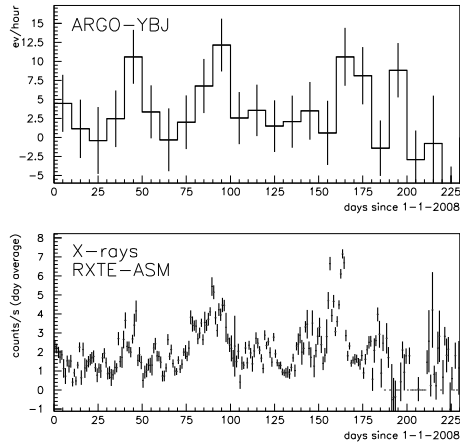
ARGO-YBJ observed the source with the whole detector installed (central carpet and sampling ring) from 2007 December 13 to 2008 August 17, for a total of 1217 on-source hours.

Fig. 8 shows the map of the Mrk421 region, obtained with the showers with  $N_{pad} \geq 40$  and  $\theta < 40^\circ$ . The significance of the signal is more than 6 standard deviations. The observed average flux is comparable with the Crab one, but the signal intensity varies with time, showing a strong correlation with the X-ray flux.

Fig.9 shows the number of events per hour with  $N_{pad} \geq 100$  (averaged over 10 days) observed by ARGO-



**FIGURE 8.** Map of the Mrk421 region from 2007 December 13 to 2008 August 17 for events with  $N_{pad} \geq 40$ . The colour scale shows the significance of the signal in standard deviations.



**FIGURE 9.** Correlation with X-rays during 230 days in 2008. Upper panel: number of events detected by ARGO-YBJ with  $N_{pad} \geq 100$ , as a function of time. Lower panel: daily-averaged X-ray counting rate detected by RXTE-ASM.

YBJ in a circular window of radius  $0.9^\circ$  around the source, as a function of time, compared to the day-average counting rate of the All Sky Monitor detector aboard the RXTE satellite, in the 1.5-12 KeV energy range[5]. The median energy corresponding to events with  $N_{pad} \geq 100$  is  $E = 2.4$  TeV.

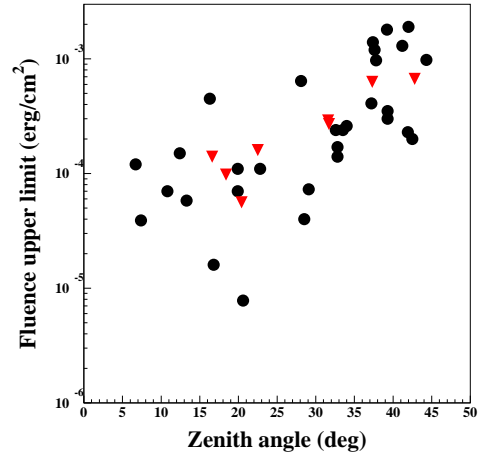


**FIGURE 10.** Fluence upper limits for 39 GRBs in the energy range 1-100 GeV, as a function of the zenith angle. The absorption of gamma rays in the intergalactic space has been taken into account using for any GRB the measured redshift when available (red triangles) or assuming  $z=1$  when the distance is unknown (black circles).

## GAMMA RAY BURSTS

The scaler mode technique[6] is a unique tool for ground based experiments to study Gamma Ray Bursts (GRBs) in the GeV energy range, where gamma rays are less affected by the absorption due to pair production in the extragalactic space.

The search has been done in coincidence with 39 GRBs detected by satellites, from December 2004 to June 2008, with the detector surface increasing from  $\sim 693$  to  $\sim 6628$  m<sup>2</sup>. Among these events, 34 belong to the so called “long GRB” class, (i.e. the time duration is  $T > 2$  s), and 5 are “short” ( $T < 2$  s).

For each GRB, the search has been done by looking for an excess of the single particle counting rate during the T90 time, i.e. during the time where the satellite instruments detected 90% of the emission.

No excess has been found in coincidence with any satellite observation.

Fig. 10 shows the fluence upper limits (99% confidence level) in the energy range 1-100 GeV obtained for the 39 GRBs, as a function of the zenith angle [7].

The upper limits have been calculated assuming a GRB power law spectrum with a differential index  $\alpha = -2.5$ , corrected by an exponential factor to account for the extragalactic absorption. The absorption factor has been evaluated according to [8], using the measured redshift when available (in 8 cases), otherwise setting the redshift  $z=1$ .

## CONCLUSIONS

ARGO-YBJ has been completely installed and since November 2007 is taking data with a duty cycle  $\geq 85\%$ .

The data recorded in the first 8 months of measurement have been analyzed in order to test the performance of the detector in the gamma ray astronomy field.

The detection of the Moon and Sun shadows, and the observation of gamma rays from the Crab Nebula and Mrk421 show that the detector is properly working, with excellent angular resolution and sensitivity.

The Crab nebula has been observed with a statistical significance of  $\sim 6$  standard deviations in 194 days, at a median gamma ray energy of  $\sim 1.1$  TeV.

Mrk421 has been detected with a statistical significance of  $\sim 6$  standard deviations in two flaring periods: in summer 2006 (during the debugging phase of the central carpet) and in the first 8 months of 2008. In particular the 2008 data show a strong variability, and a correlation with the X-ray emission has been observed during the whole period.

Working in “scaler mode” ARGO-YBJ has performed a search for emission from GRBs in coincidence with 39 events observed by satellites, setting upper limits on the fluence between  $8 \times 10^{-6}$  and  $2 \times 10^{-3}$  erg cm $^{-2}$  in the 1-100 GeV energy range.

An increase of the sensitivity in shower mode to gamma rays sources is expected with the installation of a layer of lead above the detector, and after the implementation of an offline procedure to reject a fraction of the cosmic ray background, based on the different topological pattern of hadronic and electromagnetic showers.

## REFERENCES

1. G. Aielli et al., *NIM* **A562**, 92 (2006).
2. G. Di Sciascio et al. *Proc. 30th Int. Cosmic Rays Conference* (2007).
3. H.H. He et al., *Astroparticle Physics* **27**, 528–532 (2007).
4. M. Dattoli et al., *Proc. 30th Int. Cosmic Rays Conference* (2007).
5. <http://xte.mit.edu/>
6. S. Vernetto, *Astroparticle Physics* **13**, 75–86 (2000).
7. G. Aielli et al., *Astroparticle Physics* **30**, 85–95 (2008).
8. T.M. Kneiske et al., *Astronomy and Astrophysics* **413**, 807 (2004).